

## Synthesis and properties of *c*-axis oriented epitaxial MgB<sub>2</sub> thin films

S. D. Bu, D. M. Kim, J. H. Choi, J. Giencke, E. E. Hellstrom, D. C. Larbalestier, S. Patnaik, L. Cooley, and C. B. Eom<sup>a)</sup>

*Department of Materials Science and Engineering, and Applied Superconductivity Center, University of Wisconsin-Madison, Madison, Wisconsin 53706*

J. Lettieri and D. G. Schlom

*Department of Materials Science and Engineering, Pennsylvania State University, University Park, Pennsylvania 16802*

W. Tian and X. Q. Pan

*Department of Materials Science and Engineering, University of Michigan-Ann Arbor, Ann Arbor, Michigan 48109*

(Received 1 April 2002; accepted for publication 26 June 2002)

We report the growth and properties of epitaxial MgB<sub>2</sub> thin films on (0001) Al<sub>2</sub>O<sub>3</sub> substrates. The MgB<sub>2</sub> thin films were prepared by depositing boron films via radio-frequency (rf) magnetron sputtering, followed by a postdeposition anneal at 850 °C in magnesium vapor. X-ray diffraction and cross-sectional transmission electron microscopy reveal that the epitaxial MgB<sub>2</sub> films are oriented with their *c*-axis normal to the (0001) Al<sub>2</sub>O<sub>3</sub> substrate with a 30° rotation in the (0001) plane with respect to the substrate. The critical temperature was found to be 35 K and the anisotropy ratio,  $H_{c2}^{\parallel}/H_{c2}^{\perp}$ , was about 3 at 25 K. The critical current densities at 4.2 and 20 K (at 1 T perpendicular magnetic field) are  $5 \times 10^6$  and  $1 \times 10^6$  A/cm<sup>2</sup>, respectively. The controlled growth of epitaxial MgB<sub>2</sub> thin films opens a new avenue in both understanding superconductivity in MgB<sub>2</sub> and technological applications. © 2002 American Institute of Physics. [DOI: 10.1063/1.1504490]

The discovery of superconductivity at 39 K in MgB<sub>2</sub><sup>1</sup> offers the possibility of a new class of high-speed superconducting electronic devices due to its favorable combination of higher critical temperature than conventional BCS superconductors and a symmetric order parameter (unlike HTS). It also stimulated a flurry of activity to explore the phenomenology and basic mechanism of superconductivity in this surprising material. MgB<sub>2</sub> possesses a number of attractive properties, including strongly coupled grain boundaries.<sup>2</sup> Several unusual phenomena, such as temperature-dependent electronic anisotropy<sup>3</sup> and multiple superconducting gap structures,<sup>4,5</sup> appear to distinguish MgB<sub>2</sub> from a conventional BCS superconductor, and remain to be explained.

A critical step for studying both intrinsic superconducting properties and the possibility of superconducting devices based on MgB<sub>2</sub> is the controlled growth of high quality epitaxial MgB<sub>2</sub> thin film heterostructures. The growth of MgB<sub>2</sub> films by means of both *in situ* and *ex situ* processes has been demonstrated,<sup>6–15</sup> including (0001) fiber-textured MgB<sub>2</sub> films.<sup>7</sup> Kang *et al.* reported the growth of both *c*-axis and (101)-oriented MgB<sub>2</sub> epitaxial thin films on (1 $\bar{1}$ 02) Al<sub>2</sub>O<sub>3</sub> and (100) SrTiO<sub>3</sub> substrates.<sup>6</sup> However, the reported x-ray data do not show in-plane epitaxy, and there is no clear relationship between the MgB<sub>2</sub> film orientation and the orientation of the substrate, which must be present if epitaxial control over the film growth had been attained.

In this letter, we report the growth and properties of epitaxial MgB<sub>2</sub> thin films on (0001) Al<sub>2</sub>O<sub>3</sub> substrates. In the time since we first reported the epitaxial growth of MgB<sub>2</sub> on thin films (0001) Al<sub>2</sub>O<sub>3</sub>,<sup>13</sup> two other groups have also

achieved its epitaxial growth.<sup>14,15</sup> Although MgB<sub>2</sub> has a mismatch with Al<sub>2</sub>O<sub>3</sub> of ~23% along the [11 $\bar{2}$ 0] axis, which is unfavorable for epitaxial growth, a 30° in-plane rotation of the [11 $\bar{2}$ 0] direction of the MgB<sub>2</sub> film with respect to the substrate results in a parallel orientation of [11 $\bar{2}$ 0] MgB<sub>2</sub> and [10 $\bar{1}$ 0] Al<sub>2</sub>O<sub>3</sub>. This provides a lattice mismatch of ~11%.

The MgB<sub>2</sub> thin films were prepared by depositing boron via rf magnetron sputtering, followed by a postdeposition anneal at 850 °C in the presence of magnesium vapor. Deposition was carried out at 5 mTorr argon at 500 °C using a pure boron target. The thickness of the boron films was 230 nm. The films were annealed in an evacuated quartz tube using a tantalum envelope for 5 h. The quartz tube was filled with 7–10 Torr of argon gas after evacuation to reduce the Mg loss. The film thickness increased by a factor of 1.8 during the annealing, resulting in a final thickness of 400 nm, which was confirmed by cross-sectional transmission electron microscopy (TEM). Atomic force microscopy (AFM) imaging revealed a smooth surface morphology with a rms roughness of ~3 nm. The chemical composition was obtained using wavelength dispersive x-ray spectroscopy (WDS), showing a Mg:B:O:C atomic ratio of 34.1 : 58.4 : 4.3 : 3.2, respectively. By assuming that the carbon resides on boron sites and oxygen consumes magnesium to form MgO, the Mg:B ratio of film 1 was found to be 1:2.07, which is close to the MgB<sub>2</sub> stoichiometry.

The epitaxial relationships and the crystalline quality of the MgB<sub>2</sub> thin films were assessed by four-circle x-ray diffraction. Figure 1(a) shows a  $\theta$ - $2\theta$  scan of an epitaxial MgB<sub>2</sub> thin film grown on a (0001) Al<sub>2</sub>O<sub>3</sub> substrate. The only substantial MgB<sub>2</sub> peaks are the 0001 and 0002 reflections, which clearly shows that the MgB<sub>2</sub> is oriented with its *c*-axis

<sup>a)</sup>Author to whom correspondence should be addressed; electronic mail: eom@enr.wisc.edu

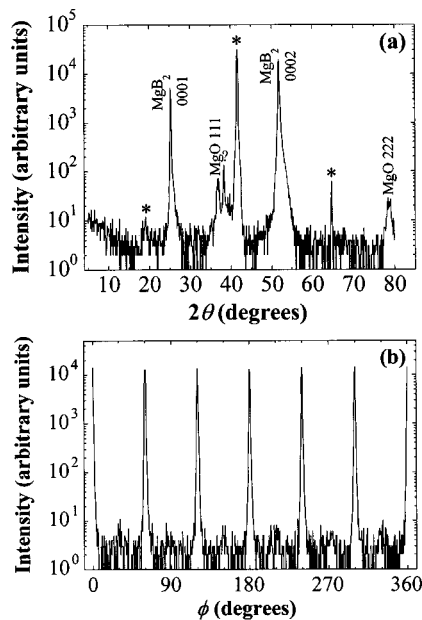


FIG. 1. X-ray diffraction scans of an epitaxial  $\text{MgB}_2$  thin film grown on a (0001)  $\text{Al}_2\text{O}_3$  substrate (a)  $\theta$ - $2\theta$  scan and (b)  $\phi$  scan of the  $10\bar{1}1$   $\text{MgB}_2$  reflection. The  $\text{Al}_2\text{O}_3$  substrate peaks are marked as \*.  $\phi=0^\circ$  is aligned to be parallel to the  $[11\bar{2}0]$  in-plane direction of the  $\text{Al}_2\text{O}_3$  substrate. The FWHM of the 0002  $\text{MgB}_2$  peak is  $0.28^\circ$  in  $2\theta$  and  $0.54^\circ$  in  $\omega$  (rocking curve). These scans indicate that the lattice constants of this  $\text{MgB}_2$  film (film 2) are  $a=3.08\pm 0.02 \text{ \AA}$  and  $c=3.52\pm 0.01 \text{ \AA}$ .

normal to the substrate. The rocking curve full width at half maximum (FWHM) of the 0002  $\text{MgB}_2$  reflection is  $0.54^\circ$ , which indicates that the crystalline quality of the film is good. We also investigated the in-plane texture of the film by scanning an off-axis peak. Figure 1(b) shows the azimuthal  $\phi$  scan of the  $\text{MgB}_2$   $10\bar{1}1$  reflection. The significant intensities every  $60^\circ$  of this reflection confirm that the film contains a single hexagonal texture in the film plane. Furthermore, the  $\text{MgB}_2$  reflections are rotated  $30^\circ$  in the basal plane with respect to the  $\text{Al}_2\text{O}_3$  lattice, resulting in a relationship between the substrate and  $\text{MgB}_2$  film of  $[11\bar{2}0]\text{MgB}_2\parallel[10\bar{1}0]\text{Al}_2\text{O}_3$ . The measured FWHM of the azimuthal  $\phi$  scan of the  $10\bar{1}1$  reflection is  $1.0^\circ$ . The  $c$ -axis lattice parameter determined from normal  $\theta$ - $2\theta$  scans is  $3.52\pm 0.01 \text{ \AA}$ , which is the same as the bulk value.<sup>1</sup>

The microstructure has been studied by cross-sectional TEM. Figure 2(a) is a low magnification bright field TEM image of a  $4000 \text{ \AA}$  thick  $\text{MgB}_2$  film grown on a (0001)  $\text{Al}_2\text{O}_3$  substrate. Figures 2(b) and 2(c) are the selected-area electron diffraction (SAED) pattern taken from the film and the substrate, respectively. Epitaxial growth of  $\text{MgB}_2$  is evident and no grain boundaries are seen in the film. The high-resolution TEM (HRTEM) image in Fig. 2(d) shows distinct interface layers of  $\text{MgAl}_2\text{O}_4$  and  $\text{MgO}$  between the  $\text{MgB}_2$  and  $\text{Al}_2\text{O}_3$ . The HRTEM image clearly shows that both  $\text{MgAl}_2\text{O}_4$  and  $\text{MgO}$  grow epitaxially on the (0001)  $\text{Al}_2\text{O}_3$ , with an orientation relationship of  $(111)[1\bar{1}0]\text{MgO}\parallel(111)[1\bar{1}0]\text{MgAl}_2\text{O}_4\parallel(0001)[10\bar{1}0]\text{Al}_2\text{O}_3$ . Additional details of TEM studies are given elsewhere.<sup>16</sup>

The transition temperature was measured with a SQUID magnetometer in a magnetic field of 5 mT, applied parallel to the film surface. Figure 3 shows an extremely sharp transition with onset at 35 K with full shielding. The 10% to 90% width of the inductive transition is  $\sim 1 \text{ K}$ , which is similar to

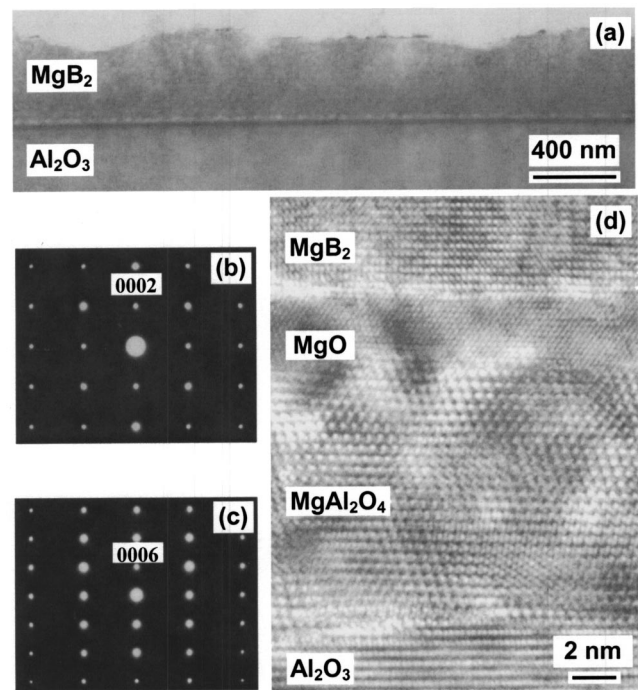


FIG. 2. (a) Bright-field cross-sectional TEM image of a  $4000 \text{ \AA}$  thick  $\text{MgB}_2$  thin film grown on a (0001)  $\text{Al}_2\text{O}_3$  substrate, (b) SAED of  $\text{MgB}_2$  along the  $[11\bar{2}0]$  zone axis, (c) SAED of  $\text{Al}_2\text{O}_3$  substrate along the  $[10\bar{1}0]$  zone axis, and (d) cross-sectional HRTEM micrograph of an epitaxial  $\text{MgB}_2$  thin film near the (0001)  $\text{Al}_2\text{O}_3$  substrate.

inductive transitions for the best bulk and single crystal samples made so far.<sup>17</sup>

The resistance was measured by a standard four-point technique in magnetic fields up to 9 T as a function of temperature. Figure 4 shows the zero field resistive transition, which indicates  $\rho(40 \text{ K})=6.5 \mu\Omega \text{ cm}$  and a residual resistance ratio (RRR) of  $\sim 2$ . We also measured the in-field transitions for field applied parallel to the  $c$  axis and to the  $ab$  plane of the film. The in-field resistive transitions exhibit very little broadening up to the highest field measured (9 T), unlike our earlier measurements on fiber-textured films.<sup>3</sup> The upper critical field was defined for parallel ( $H_{c2}^{\parallel}$ ) and perpendicular ( $H_{c2}^{\perp}$ ) fields by extrapolating the steep part of the transition to the normal state resistance.<sup>3</sup> The inset to Fig. 4 shows the upper critical field versus temperature. The anisotropy ratio,  $H_{c2}^{\parallel}/H_{c2}^{\perp}$ , is about 3 at 25 K, rather greater than film<sup>3,18</sup> and single crystal values.<sup>17</sup> At low temperatures, the nearly parallel trends and similar slopes of  $H_{c2}^{\parallel}(T)$  and  $H_{c2}^{\perp}(T)$  suggest decreasing anisotropy with decreasing temperature, a trend which is opposite to some recent data.<sup>19,20</sup> It

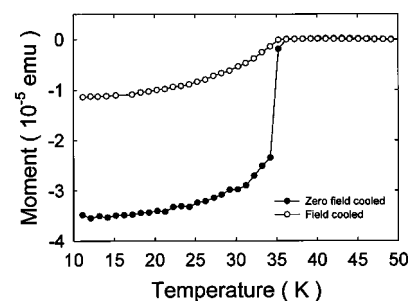


FIG. 3.  $T_c$  data obtained with a SQUID magnetometer utilizing a 5 mT magnetic field applied parallel to the film surface.

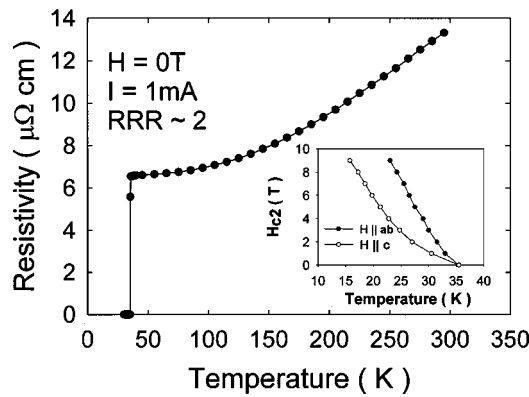


FIG. 4. Resistivity vs. temperature of MgB<sub>2</sub> thin film. The inset shows the  $H_{c2}$  for fields applied parallel and perpendicular to the crystal axes.

is clear that there is as yet no convergence on what the upper critical field anisotropy of MgB<sub>2</sub> is.

The critical current density,  $J_c$ , was determined by magnetization measurements using a vibrating sample magnetometer in the field range of 0–12 T. Figure 5 shows  $J_c$  vs. magnetic field at 4.2 and 20 K in a perpendicular magnetic field. To estimate  $J_c$ , we used the standard expression for the critical state of a thin film with rectangular area,<sup>21</sup>  $J_c = 2\Delta M(12b)/(3b-d)d$ , where  $b=4.5$  mm and  $d=3.0$  mm are the film dimensions and  $\Delta M$  is the total magnetization hysteresis measured from the field increasing and field decreasing branches of the magnetization curve. This analysis yields  $J_c$  values of  $4.5 \times 10^6$  A/cm<sup>2</sup> at 4.2 K and 1 T, and  $1 \times 10^6$  A/cm<sup>2</sup> at 20 K and 1 T. These values contrast the almost reversible behavior of bulk single crystals<sup>14</sup> and are significantly larger than the values obtained from polycrystalline bulk forms of MgB<sub>2</sub>,<sup>2,22,23</sup> where grain boundary flux pinning is often thought to be operating. In this case grain boundaries cannot be responsible for the flux pinning, but it is evidently still very strong. We assume that some site interchange disorders must be contributing to the flux pinning.

In conclusion, we have demonstrated the growth of epitaxial MgB<sub>2</sub> films with high crystalline quality and high  $J_c$ . Although the films are epitaxial, the properties are distinctively different from bulk single crystals in terms of their very strong flux pinning and suppressed  $T_c$ . We attribute this to alloying of the MgB<sub>2</sub> film by impurity atoms or some other defects. The growth of epitaxial MgB<sub>2</sub> thin films with

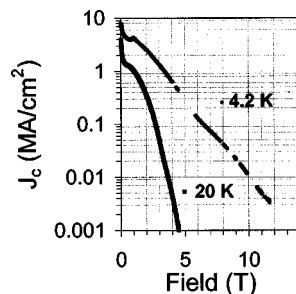


FIG. 5. Critical current density vs magnetic field measured using a vibrating sample magnetometer at 4.2 and 20 K in a perpendicular magnetic field. Deviations below 1 T are associated with the lack of full flux penetration and actual  $J_c$  values are higher.

controlled orientations and properties opens a new avenue to understand the superconductivity in MgB<sub>2</sub> and potential applications for both electronic devices and high field magnets.

The work at the University of Wisconsin was supported by National Science Foundation through the MRSEC for Nanostructure Materials. The authors are grateful to A. Gurevich for discussions. X.Q.P. gratefully acknowledges the financial support of the National Science Foundation through Grant Nos. DMR 9875405 (CAREER) and DMR/IMR 9704175.

- <sup>1</sup>J. Nagamatsu, N. Nakagawa, T. Muranaka, Y. Zenitani, and J. Akimitsu, *Nature* (London) **410**, 63 (2001).
- <sup>2</sup>D. C. Larbalestier, L. D. Cooley, M. O. Rikel, A. A. Polyanskii, J. Jiang, S. Patnaik, X. Y. Cai, D. M. Feldmann, A. Gurevich, A. A. Squitieri, M. T. Naus, C. B. Eom, E. E. Hellstrom, R. J. Cava, K. A. Regan, N. Rogado, M. A. Hayward, T. He, J. S. Slusky, P. Khalifah, K. Inumaru, and M. Haas, *Nature* (London) **410**, 186 (2001).
- <sup>3</sup>S. Patnaik, L. D. Cooley, A. Gurevich, A. A. Polyanskii, J. Jing, X. Y. Cai, A. A. Squitieri, M. T. Naus, M. K. Lee, J. H. Choi, L. Belenky, S. D. Bu, J. Letteri, X. Song, D. G. Schlom, S. E. Babcock, C. B. Eom, E. E. Hellstrom, and D. C. Larbalestier, *Supercond. Sci. Technol.* **14**, 315 (2001).
- <sup>4</sup>P. Szabo, P. Samuely, J. Kacmarcik, T. Klein, J. Marcus, D. Fruchart, S. Miraglia, C. Marcenat, and A. G. M. Jansen, *Phys. Rev. Lett.* **8713**, 7005 (2001).
- <sup>5</sup>F. Giubileo, D. Roditchev, W. Sacks, R. Lamy, D. X. Thanh, J. Klein, S. Miraglia, D. Fruchart, J. Marcus, and P. Monod, *Phys. Rev. Lett.* **8717**, 7008 (2001).
- <sup>6</sup>W. N. Kang, H. J. Kim, E. M. Choi, C. U. Jung, and S. L. Lee, *Science* **292**, 1521 (2001).
- <sup>7</sup>C. B. Eom, M. K. Lee, J. H. Choi, L. J. Belenky, X. Song, L. D. Cooley, M. T. Naus, S. Patnaik, J. Jiang, M. Rikel, A. Polyanskii, A. Gurevich, X. Y. Cai, S. D. Bu, S. E. Babcock, E. E. Hellstrom, D. C. Larbalestier, N. Rogado, K. A. Regan, M. A. Hayward, T. He, J. S. Slusky, K. Inumaru, M. K. Haas, and R. J. Cava, *Nature* (London) **411**, 558 (2001).
- <sup>8</sup>D. H. A. Blank, H. Hilgenkamp, A. Brinkman, D. Mijatovic, G. Rijnders, and H. Rogalla, *Appl. Phys. Lett.* **79**, 394 (2001).
- <sup>9</sup>X. X. Xi, Y. Zhang, A. Soukiassian, J. Jones, J. Hotchkiss, Y. Zhong, C. O. Brubaker, Z.-K. Liu, J. Lettieri, D. G. Schlom, Y. F. Hu, E. Wertz, Q. Li, W. Tian, H. P. Sun, and X. Q. Pan, *Supercond. Sci. Technol.* **15**, 451 (2002).
- <sup>10</sup>H. Y. Zhai, H. M. Christen, L. Zhang, A. Paranthaman, C. Cantoni, B. C. Sales, P. H. Fleming, D. K. Christen, and D. H. Lowndes, *J. Mater. Res.* **16**, 2759 (2001).
- <sup>11</sup>K. Ueda and M. Naito, *Appl. Phys. Lett.* **79**, 2046 (2001).
- <sup>12</sup>J.-U. H. W. Jo, T. Ohnishi, A. F. Marshall, M. R. Beasley, and R. H. Hammond, Presented at the MRS Fall Meeting (2001).
- <sup>13</sup>C. B. Eom *et al.*, presented at the MRS Fall Meeting (2001).
- <sup>14</sup>A. Berenov, Z. Lockman, X. Qi, J. L. MacManus-Driscoll, Y. Bugoslavsky, L. F. Cohen, M.-H. Jo, N. A. Stelmashenko, V. N. Tsaneva, M. Kambara, N. Hari Babu, D. A. Cardwell, and M. G. Blamire, *Appl. Phys. Lett.* **79**, 4001 (2001).
- <sup>15</sup>X. H. Zeng, A. V. Pogrebnyakov, A. Kotcharov, J. E. Jones, X. X. Xi, E. M. Lysczek, J. M. Redwing, S. Y. Xu, Qi Li, J. Lettieri, D. G. Schlom, W. Tian, X. Q. Pan, and Z. K. Liu, *Nature Materials* (to be published).
- <sup>16</sup>W. Tian, X. Q. Pan, S. D. Bu, D. M. Kim, J. H. Choi, S. Patnaik, and C. B. Eom, *Appl. Phys. Lett.* **81**, 685 (2002).
- <sup>17</sup>M. Xu, H. Kitazawa, Y. Takano, J. Ye, K. Nishida, H. Abe, A. Matsushita, N. Tsujii, and G. Kido, *Appl. Phys. Lett.* **79**, 2779 (2001).
- <sup>18</sup>C. Buzea and T. Yamashita, *Supercond. Sci. Technol.* **14**, R115 (2001).
- <sup>19</sup>S. L. Yu, E. L. Eltsev, K. Nakao, N. Chikumoto, S. Tajima, N. Koshizuka, and M. Murakami, *cond-mat/0201451*.
- <sup>20</sup>M. Angst, R. Puzniak, A. Wisniewski, J. Jun, S. M. Kazakov, J. Karpinski, J. Roos, and H. Keller, *Phys. Rev. Lett.* **88**, 167004 (2002).
- <sup>21</sup>J. Evetts, *Concise Encyclopedia of Magnetic and Superconducting Materials* (Pergamon, New York, 1992), p. 99.
- <sup>22</sup>D. K. Finnemore, J. E. Ostenson, S. L. Bud'ko, G. Lapertot, and P. C. Canfield, *Phys. Rev. Lett.* **86**, 2420 (2001).
- <sup>23</sup>G. Grasso, A. Malagoli, C. Ferdeghini, S. Roncallo, V. Braccini, A. S. Siri, and M. R. Cimberle, *Appl. Phys. Lett.* **79**, 230 (2001).